American Mineralogist, Volume 89, pages 1240–1246, 2004

Investigation of jet breakup and droplet size distribution of liquid CO_2 and water systems—implications for CO_2 hydrate formation for ocean carbon sequestration

David Riestenberg, Elizabeth Chiu, Monsuru Gborigi, Liyuan Liang, Olivia R. West, and Costas Tsouris*

Oak Ridge National Laboratory, P. O. Box 2008, Oak Ridge, Tennessee 37831-6181, U.S.A.

Abstract

An experimental investigation has been conducted into the effect of fluid velocity and orifice size on the breakup patterns of liquid CO_2 in water, as well as those for water in CO_2. Under high-pressure and low-temperature conditions, the jet breakup patterns follow distinct Rayleigh, transitional, and spray modes. Droplet size distribution was determined in the different modes, with the spray mode producing the smallest droplets and the most uniform size distribution. The system appears to progress from transitional to spray mode when the Ohnesorge number is approximately 18 Re^{-1}. Using this relationship, it is possible to predict the minimum injection rate necessary for spray mode at any injector diameter. Under hydrate-forming conditions, the jet breakup did not appear to be affected because breakup occurred faster than hydrate formation. However, injection into a confined space could promote droplet coalescence, resulting in a larger average drop size. These results can be used to control hydrate conversion in an ocean CO_2 injection system and to ensure a large dispersion of injected CO_2 during its sequestration in the ocean.

Introduction

During the 20th century, the atmospheric concentration of CO_2 increased by over 20% (Siegenthaler and Sarmiento 1993) and is predicted to continue to increase throughout the 21st century. If measures are not taken to reduce anthropogenic CO_2 emissions into the atmosphere, the buildup of this greenhouse gas is predicted to result in global warming over the next 100 years, a phenomenon that may already be causing impacts on the Earth's climate and weather (Watson 2001). Therefore, it is necessary to reduce the rate of CO_2 emissions in the atmosphere until technological improvements in energy generation can slow down CO_2 production. Improvements in alternative energy sources, such as wind, solar, and nuclear, are not sufficient in the short term to keep the concentration of CO_2 sufficiently low to prevent a potentially profound impact on the Earth's climate. Hence, energy improvements must be coupled with carbon sequestration technologies to control atmospheric CO_2 concentrations over at least the next 20 to 40 years (Medina et al. 2001). The deep ocean is one location being considered for CO_2 sequestration.

Intermediate and deep ocean waters (≥500 m) present some advantages over other potential locations currently being investigated (i.e., terrestrial and geologic) to sequester CO_2 from the atmosphere. First, these ocean waters contain a total storage capacity of up to 40,000 Gt of carbon (95% of this in the deep ocean), while annual anthropogenic emissions of carbon are expected to range from 7.4 to 26 Gt, increasing over the next 100 years (U.S. Department of Energy 1999). In comparison, the atmospheric concentration of carbon has increased from approximately 600 to 750 Gt over the past 100 years (Ormerod et al. 2002; Ametistova et al. 2002). Second, ocean waters have been the major sink for global CO_2 over geologic time and it appears that the ocean is absorbing more CO_2 than any other natural sink, up to one third of the current anthropogenic contribution (Ormerod et al. 2002). However, this CO_2 is entering the biologically rich shallow ocean prior to its longer-term storage, during which period it slowly exchanges with the undersaturated deeper waters, where it may be stored for periods of around 1000 years (Adams et al. 1995). Injection of CO_2 as an extended, negatively buoyant plume that passes into these deeper waters could potentially bypass the damaging effects caused by the current fluxes of atmospheric CO_2 entering the shallow ocean (Kleypas et al. 1999) or the effects that direct deep injection may have on the biota of the deep ocean (Seibel and Walsh 2001).

Another important advantage of ocean CO_2 sequestration over other potential storage options, such as geologic sequestration, is its minimal potential for risk. Ocean waters disperse CO_2 rapidly, so the risk for massive CO_2 release is low. On the other hand, injections into geologic formations may lead to storage of CO_2 at high concentrations and, quite possibly, near inhabited areas. A sudden release of CO_2 from a geologic reservoir may lead to dangerous atmospheric conditions for humans and other biota in the proximity of the injection.

Liquid-in-liquid jet instability has been recognized as an important process in CO_2 sequestration in the deep ocean (Teng et al. 1995; Tang et al. 2002; Lee et al. 2003). In direct injection of liquid CO_2 into seawater, interfacial instability causes CO_2 droplets to form following jet breakup (Teng et al. 1995). The breakup pattern and the size distribution of the CO_2 droplets are important for assessing the impact on the marine environment, because CO_2 dissolution, dispersion, and the subsequent acidification of seawater are closely related to droplet sizes (Tang et al. 2002). Because smaller droplets have a higher surface-to-volume ratio,

* E-mail: tsourisc@ornl.gov

0003-004X/04/0809–1240$05.00

mass transfer and reaction rates can be significantly increased as droplet size decreases (Teng and Zhao 1999). This phenomenon has also been suggested as a means of increasing conversion of CO_2 to CO_2 hydrate in experiments in which water droplets were sprayed into a stream of liquid CO_2 in order to produce sinking hydrate-containing particles for direct ocean injection (Lee et al. 2003; West et al. 2003; Tsouris et al. 2004).

While jet instability and breakup have been extensively investigated for liquid-in-gas systems (e.g., water jet in air) (Weber 1931), liquid-in-liquid jet breakup is poorly understood (Tang et al. 2002). Unlike liquid-in-gas systems, where the jets usually produce droplets of uniform size as a result of capillary instability, droplets produced in liquid-in-liquid systems are often not very uniform (Teng et al. 1995). The pattern of droplet formation depends on the velocity of the jet and the physical properties of the continuous and injected fluids. However, if jet breakup is in the Rayleigh regime, the average diameter of droplets (d) in a liquid-liquid system can be calculated independently of injection velocity, as a ratio of orifice diameter (d_0) and is a function of the Ohnesorge number, Z [$Z = \mu_d/(\rho\sigma d_0)^{0.5}$]. Teng et al. (1995) introduced a modified Ohnesorge number and developed the relationship:

$$\frac{d}{d_0} = \left(\frac{3\pi}{\sqrt{2}}\right)^{1/3} \left(1 + Z^*\right)^{1/6} \tag{1}$$

where the dimensionless number Z^* is defined as

$$Z^* = (3\mu_d + \mu_a) / (d_0\sigma\rho)^{1/2} \tag{2}$$

where μ_d and μ_a are the dynamic viscosities (g/cm·s) of the dispersed and ambient liquids (denoted by subscripts d and a, respectively), σ is the interfacial tension between the two phases, and ρ is the density of the dispersed liquid. Viscosities and densities were calculated using the NIST Chemistry Webook Database (Lemmon et al. 2003). The interfacial tension for a water-CO_2 system over the range of temperatures and pressures in this study was provided by linear double interpolation of the values of Chun and Wilkinson (1995).

For liquid-in-liquid jet breakup, drop size may be calculated with Equation 1, derived on the basis of Rayleigh's maximum instability theory. Equation 1 applies to both liquid-in-liquid and liquid-in-gas systems, provided the jet velocity is low (Teng et al. 1995). As the injection velocity increases, Kitamura et al. (1982) found that the surface disturbance wave on the jet becomes irregular, producing nonuniform droplet sizes. If the injection rate is sufficiently high, atomization of the jet is observed (Teng and Zhao 1999). In a study of jet breakup of CO_2 in water, results show that distinct breakup patterns exist as a function of the Reynolds and Ohnesorge numbers (Tang et al. 2002). Their study provided observations of liquid-in-liquid jet breakup, but more experiments are needed to quantitatively characterize the transitional-flow and turbulent-flow regimes. Little information is available on droplet size distribution during breakup of a water-in-CO_2 jet as flow changes from laminar through transitional to turbulent. Such information is relevant to processes where water and CO_2 are mixed via liquid-in-liquid jetting because reduced droplet size increases mass transfer, thus increasing hydrate conversion, if the system exists under hydrate-forming pressure and temperature conditions (Aya et al. 1997; Yamasaki et al. 2000; Lee et al. 2003). Through experimental investigation, this study aims at understanding the behavior of liquid-in-liquid jet breakup with systems of CO_2 in water and water in CO_2 under high-pressure and low-temperature conditions. Jet breakup regimes and droplet size distributions were determined under different flow conditions with varying orifice diameters.

Experimental methods

Jet breakup and droplet size observation

Experiments involving CO_2 and water jet breakup were performed in the Seafloor Process Simulator (SPS) facility at Oak Ridge National Laboratory. The SPS has been described previously (Phelps et al. 2001; West et al. 2003) (Fig. 1). The pressure vessel has an internal diameter of 0.32 m and an internal height of 0.91 m, providing a reaction volume of 72 L. It is equipped with sapphire windows, thermocouples, and pressure transducers. An 8 mm (outside diameter) by 56 cm long borescope was inserted into the vessel to allow for high magnification observations of the droplets. The sapphire windows provide access for jet breakup visualization, and a digital camera (Nikon COOLPIX 990) was used to record the behavior of the jet coming out of the injector. We used shutter speeds of 1/500 s and 1/1000 s in order to capture the droplets as they moved. To ensure that there was sufficient light for recording the images during the experiments, a focusing lens was employed to concentrate light from a fiber-optic source onto a white screen that was placed inside the vessel and situated behind the injector. A simple injector, made of stainless steel capillaries with an outside diameter (OD) of 794–1588 μm and an inside diameter (ID) of 127–508 μm was used. The injector was inserted into the vessel vertically. During experiments, the internal temperature, pressure, and flow rate were monitored and recorded. Jet breakup behavior was also observed and recorded.

At the start of the CO_2-in-water injection experiments, the pressure vessel was filled with distilled water and cooled to the experimental temperature (10.0–12.0 °C). The vessel was pressurized with nitrogen gas up to experimental pressures (5.5–6.2 MPa, corresponding to depths of 550–620 meters respectively in the ocean). At these pressures, CO_2 hydrate is not expected to form above 10.6 ºC (Sloan 1998). Throughout the injection experiments, the pressure in the SPS was relatively constant due to the large headspace volume. A syringe pump (ISCO DM 100) was used to pump liquid CO_2 or water through the injector into the vessel at flow rates of 0.5–25.0 mL/min.

For the water-in-CO_2 experiments, a slightly different procedure was used. Before the start of the experiment, a clear glass column, open at the top and bottom, was placed inside the SPS between the white screen and the sapphire window. The column was square in cross section (18 mm on each side) to prevent distortion of photographic images of the drops. The SPS was then filled with distilled water and allowed to equilibrate to the desired experimental temperature. Once again, the vessel was pressurized with nitrogen gas and the pressure was held at 5.5–6.2 MPa. A volume of 300–400 mL of liquid CO_2 was first injected from the top of the vessel into the glass column, displacing the water in the column. Water was then

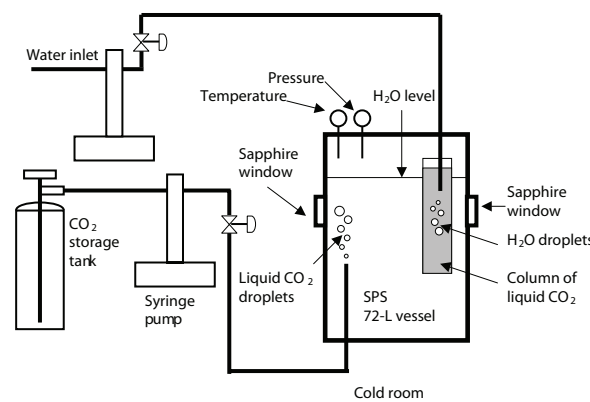

Figure 1. Schematic of the water and liquid CO_2 jet breakup experiments in the Seafloor Process Simulator (SPS).

injected through the capillary injector from the top of the vessel into the liquid CO_2 at flow rates of 0.5–25.0 mL/min.

Injection experiments of water into liquid CO_2 were also conducted under hydrate forming conditions (temperature = 4.0 °C, pressure = 5.5 MPa). Otherwise, the experimental procedure is similar to that of the CO_2-in-water injection experiment described above.

RESULTS AND DISCUSSION

Liquid-in-liquid breakup modes in non-hydrate forming conditions

Because liquid CO_2 and water are immiscible, when one liquid (dispersed phase) is injected into the ambient liquid (continuous phase), the issuing jet is hydrodynamically unstable and breaks up into droplets, either near the orifice or at the end of the jet (Teng et al. 1995). In our experiments, distinct patterns of jet breakup were observed (Fig. 2). At low injection velocities, for which the jet Reynolds number is small, a jet of the dispersed phase is formed, issuing from the nozzle. Droplets formed at the tip of the jet and broke away from the jet as individual drops (Figs. 2a and 2d). When an injector of large ID was used (381 or 508 μm), the velocity of the dispersed phase was low and large droplets were observed to form close to the tip of the nozzle (not shown in Fig. 2). The droplets that formed were relatively uniform in size. This mode of breakup, which may be described by Rayleigh's maximum instability theory and which is consistent with previous observations under low jet velocities (Meister and Scheele 1969; Kitamura et al. 1982; Tang et al. 2002), was determined visually and is referred to as the Rayleigh mode.

As the velocities of the dispersed phase increased, the jet Reynolds number increased and the uniformity of the droplets decreased (Teng and Zhao 1999; Tang et al. 2002). Large droplets of irregular shapes were observed together with smaller spherical ones (Figs. 2b and 2e). This mode of breakup is referred to as the "transitional mode."

At even higher velocities, atomization of the jet occurred in our system in a manner similar to previous observations (Teng and Zhao 1999). In this "spray" breakup mode, very fine droplets were observed to form close to the tip of the nozzle (Figs. 2c and 2f). The jet length was observed to decrease with increased flow rate, and droplets in this regime were relatively uniform in size.

Unlike the previous studies, in which the injector nozzle size ranged from 1.5 to 10 mm (Teng and Zhao 1999; Tang et al. 2002), much smaller nozzle orifices (127–508 μm) were used here. With the larger orifice size, high injection rates were needed to obtain similar droplet breakup modes (Teng and Zhao 1999). For most of the different injector capillaries used here, the three different modes of jet breakup (Rayleigh, transitional, and spray) were observed with flow rates of 0.5–25 mL/min. At a given capillary injector size, the range of flow rates that correspond to each of the distinct jet breakup pattern were determined (Table 1). The flow rates that define each breakup regime generally increase from Rayleigh through transition to spray mode, as the nozzle orifice of the capillary injector increases. However, the spray mode could not be achieved with the nozzle orifice sizes of 381 and 508 μm at the highest flow rate used (25 mL/min) (Table 1). In comparing the CO_2-in-water experiments with those of water in CO_2, little difference exists in the range of flow rates defining either water-jet or CO_2-jet breakup regimes. Although fluid properties, such as viscosity, density, and surface tension generally affect breakup patterns (Kitamura et al. 1982), the differences between these parameters (e.g., density and viscosity) for water and CO_2, especially at increased pressure (Brewer et al. 1999; Chun and Wilkinson 1995), become increasingly small. Thus, as far as jet break-up pattern is concerned, CO_2 in water would break up similarly to water in CO_2 at the experimental pressures used in this study or at higher pressures.

Images taken at different flow rates during the experiments were analyzed and assigned to one of the three breakup modes. In Figure 3, the corresponding Ohnesorge number $[Z = \mu_d/(\rho\sigma d_0)^{0.5}]$ is plotted against the jet Reynolds number ($Re = \rho U d_0/\mu_d$, where U is the velocity of dispersed liquid). The results for both the CO_2-in-water and water-in-CO_2 injection experiments are shown in Figure 3. The results of the CO_2-in-water injection experiments conducted by Tang et al. (2002), who used a much larger orifice size (2–10 mm), are also presented in the figure. These data fall in the lower right corner of the graph, indicating that higher flow

TABLE 1. Flow regimes for injection experiments

Capillary ID (μm)	Jet Breakup Flow Ranges (mL/min)		
	Rayleigh	Transition	Spray
		CO_2 injection	
127	<4	4–5	>5
178	<5	5–7	>7
254	<9	9–16	>16
381	<10	10–25	not observed
508	≤25*	not observed	not observed
		Water injection	
127	<4	4–6	>6
254	<9	9–16	>16
508	≤25*	not observed	not observed

* Maximum flow rate used was 25 mL/min.

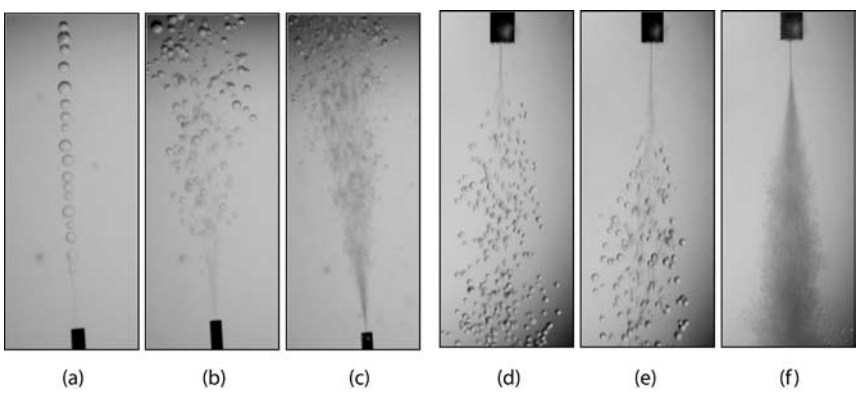

FIGURE 2. (**a**–**c**) Visualization of different jet breakup regimes in CO_2 injection experiments. Internal diameter of capillary = 178 μm, external diameter of capillary = 794 μm, system temperature = 11.0 °C, system pressure = 845 psi. (**a**) Rayleigh, (**b**) transitional, (**c**) spray. (**d**-**f**) Visualization of different jet breakup regimes in H_2O injection experiments. Internal diameter of capillary = 127 μm, external diameter of capillary = 1587 μm, system temperature = 11.5 °C, system pressure = 847 psi. (**d**) Rayleigh, (**e**) transitional, (**c**) spray.

rates (as reflected in higher *Re*) were required to obtain CO_2 jet breakup with large orifice size, similar to the observation by Teng and Zhao (1999). There may be some error in calculation of the *Z* and *Re* values for this study since the physical properties of the fluids were estimated using literature values (Chun and Wilkinson 1995; Lemmon et al. 2003). However, the two data sets and that of Tang et al. (2002) form a consistent pattern, showing distinct Rayleigh, transitional, and spray breakup regimes. The data are separated by two experimentally fit lines, defined by Tang et al. (2002) as $Z = 5.5\ Re^{-1}$ and $Z = 18\ Re^{-1}$, which were obtained by visual approximation of the transitional boundaries between the breakup modes. As seen in Figure 3, at a given jet velocity (i.e., along a line of constant *Re*) and experimental conditions (*P*,*T*), which determine the physical properties of the dispersed and the continuous phase, breakup can be changed from the Rayleigh to the spray regime by decreasing the injector orifice. In effect, decreasing the orifice diameter increases the Ohnesorge number, *Z*, which represents the ratio of the effective viscous force to the interfacial force (Teng et al. 1995); thus, the interfacial force is decreased. On the other hand, for a chosen injector dimension (i.e., along a line of constant *Z*), spray or atomization can be achieved only by increasing flow rate (i.e., by increasing hydrodynamic forces). Thus, the regime boundaries obtained from experimental data in Figure 3 can be used to predict the jet breakup modes with different injector diameters and different physical properties of the continuous and injected fluids (e.g., viscosity, density, surface tension), which depend on thermodynamic conditions (temperature, pressure, etc.).

DROPLET SIZE DISTRIBUTIONS

Droplet size measurements were made for the different injectors and jet breakup modes. For a given breakup mode and capillary size, droplets were measured for several flow rates and assembled into one droplet size distribution data set. For example, for liquid CO_2 injection using the 254 μm capillary, 123 droplet measurements were made for spray-mode breakup using flows ranging from 17–25 mL/min and were then considered as one droplet size distribution data set. There was no significant droplet size change observed within a given breakup regime using the same capillary (data not shown). Figure 4 shows droplet size distributions for two different jet breakup modes for the liquid CO_2-in-water injection experiments, and Figure 5 shows comparable data for the water-in-CO_2 injection experiments. For a given capillary, the average droplet sizes were larger and the size distributions were broader in both the Rayleigh and the spray modes for the CO_2-in-water injections than for the water-in-CO_2 injections. For example, when using the 508 μm capillary, ~95% of the droplets were larger than 1000 μm for the CO_2-in-water injections (Fig. 4a), while in the water-in-CO_2 injections, 60% of the droplets were larger than 1000 μm (Fig. 5a). It was also apparent that when both systems were operating in Rayleigh mode, the droplet sizes increased with increasing capillary internal diameter in agreement with the general prediction based on Equation 1 (Teng et al. 1995; Tang et al. 2002). However, for experiments in which spray mode was observed (Figs. 4b and 5b), the droplet sizes did not appear to increase as much with the increasing capillary diameter, particularly in the water-in-CO_2 experiments. This is an important result, especially in the application of hydrate conversion under spray mode (see later discussion). It should be noted that some error may arise in the droplet size measurement due to the difficulty in detecting and

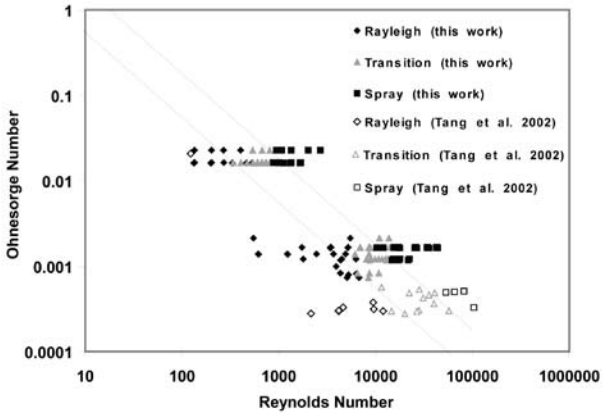

FIGURE 3. Injected fluid Reynolds number vs. Ohnesorge number for CO_2-in-water and water-in-CO_2 injections. The solid line represents the threshold between Rayleigh and transitional jet modes ($Z = 5.5\ Re^{-1}$), while the dashed line represents the threshold between transitional mode and spray mode ($Z = 18\ Re^{-1}$). The data of Tang et al. (2002), representing jet modes of CO_2 injected into water, are also shown.

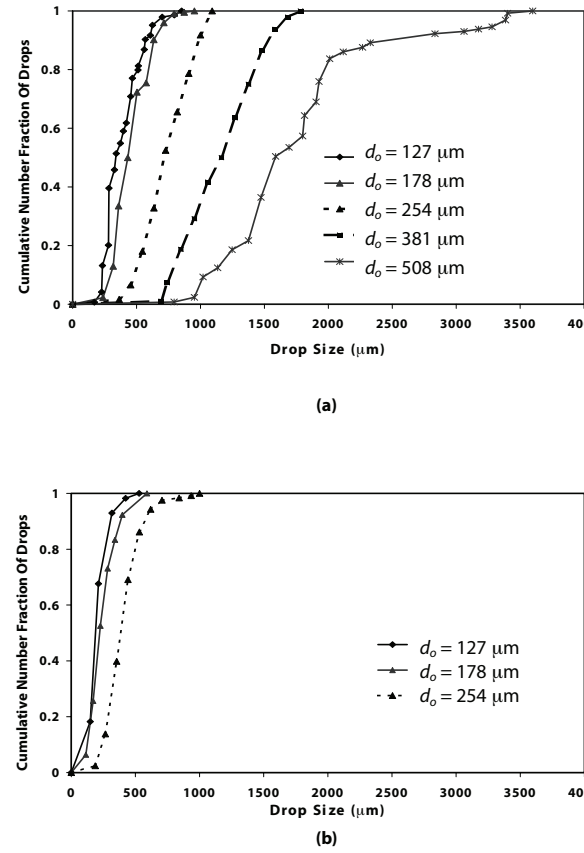

FIGURE 4. Comparisons of droplet sizes for different capillaries in CO_2 injection experiments for the flow rate ranges in Table 1. (**a**) Droplet size distributions in Rayleigh mode. (**b**) Droplet size distributions in spray mode.

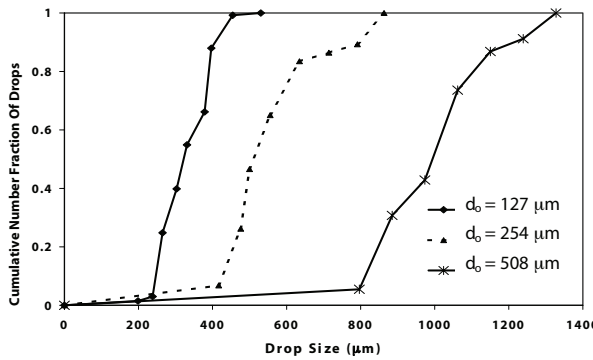

(a)

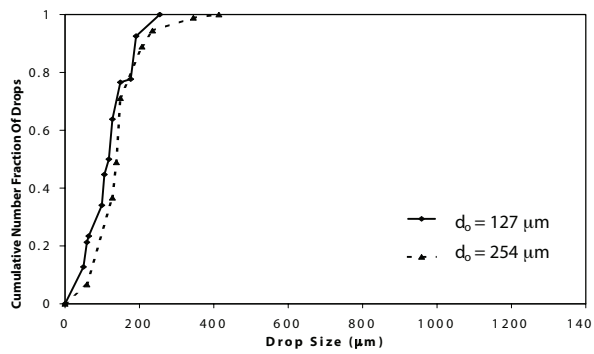

(b)

FIGURE 5. Comparisons of droplet sizes for different capillaries in water injection experiments for the flow rate ranges in Table 1. (**a**) Droplet size distributions in Rayleigh mode. (**b**) Droplet size distributions in spray mode.

measuring very small droplets produced by spray breakup.

Using Equation 1, d/d_0 values were calculated for the injection experiments and tabulated with the measured average drop size under the Rayleigh regime (Table 2). Because the Z^* factor was relatively small for all experimental conditions due to the low viscosity of both CO_2 and water, the calculated values for d/d_0 approached the limiting value of 1.88, similar to the experimental data for water jets in air (Tyler 1933). The theoretical calculation suggests that the droplet size is independent of fluid property when the fluids are of low viscosity (Teng et al. 1995).

Although experimental data show a general agreement with the theory, higher-than-predicted droplet sizes were measured (Table 2). In addition, the theory predicted larger drops for the water-in-CO_2 system than for the CO_2-in-water system while the experiments showed the reverse. The apparent inconsistencies may result from the relatively high jet velocity in our experiments which could have invalidated the application of Rayleigh's maximum instability theory. On the other hand, no general theory exists for liquid-in-liquid jet breakup and drop size associated with each breakup pattern (Teng et al. 1995; Tang et al. 2002). In general, the theoretical results based on Rayleigh's theory are almost always higher than the measured drop size in the spray mode (Table 2). Thus, the calculation provides an upper boundary on drop size in the spray regime and verifies experimental measurements at relatively low jet velocities for viscous fluids (Kitamura et al. 1982; Teng et al. 1995).

Effect of hydrate formation on water-in-CO_2 jet breakup

Water-in-CO_2 jet breakup was also conducted under hydrate-forming conditions in order to characterize the size distribution of hydrate-covered droplets and the subsequent aggregation of the droplets. Visualization of the droplets was difficult because hydrate immediately formed on the interface of the glass column, which was wetted by water droplets, after injection began. Figure 6 shows an example of hydrate-covered water droplets as they collected into a relatively cohesive mass.

Application of liquid-in-liquid injection has been used to maximize mass transfer and chemical reaction at the water and CO_2 phase boundary to increase hydrate production (West et al. 2003; Lee et al. 2003). In these previous experimental studies, water was injected into CO_2 within a coflow injector (Fig. 7a), which consisted of a capillary tube for water delivery, concentrically located within a Teflon tube used for liquid CO_2 delivery. Experiments were conducted under hydrate-forming conditions with low ambient temperatures (2–10 °C) and high pressures (10–13 MPa). With a water injection rate of 15–25 mL/min into a 127 μm capillary, jet breakup was expected to be in the spray mode as seen under the non-hydrate-forming conditions (Table 1). The measured size (267 μm) for the hydrate covered drops falls in between the droplet sizes measured in spray and transitional mode injections under non-hydrate-forming conditions (Table 2, Fig. 7b). Jet breakup could be in spray mode, but we attribute the larger size droplets to a mechanism of coalescence following jet breakup in the confined space of the coflow reactor, where an outer tube of 6.4 mm surrounds the capillary injector (West et al. 2003). Droplet coalescence would not have occurred if hydrates had formed instantaneously on the surfaces of the droplets. However, even though the thermodynamic conditions promote fast formation of hydrate Uchida et al. 1999, the high droplet concentration in the outer tube of the reactor favors collision of the droplets, and a fraction of these collisions lead to coalescence. Note that the droplet diameter predicted by Equation 1 is larger than the corresponding diameter under non-hydrate conditions (Table 2) due to changes in fluid properties under different pressure and temperature conditions.

Spray mode jet breakup is desired because this mode consistently produced droplets of the smallest diameter and the narrowest size distributions when compared with the other jet breakup modes in the water and liquid CO_2 systems (Table 2). Minimizing the droplet size results in the maximum interfacial area between water and CO_2, an important factor in the conversion of CO_2 to hydrate (Aya et al. 1997; Yamasaki et al. 2000; West et al. 2003; Lee et al. 2003). Both the water and CO_2 systems appear to progress from transitional mode to spray mode following the relationship $Z \geq 18\ Re^{-1}$ (Fig. 3, Tang et al. 2002). Using this relationship, the water injection rate necessary to achieve spray mode may be calculated for any injector diameter and under a given set of operating conditions (P, T).

IMPLICATIONS

Liquid-liquid jet breakup experiments show distinct breakup regimes, which are defined by boundaries in the graph of Oh-

TABLE 2. Measured average droplet size (d) under different jet breakup regimes, compared with the theoretically calculated droplet size using Rayleigh's maximum stability theory (Teng et al. 1995)

Capillary d_0 (μm)	μ_d (g/cm·s)	μ_c (g/cm·s)	σ (mN/m)	ρ (g/cm³)	Z	d/d_0	Calculated d (μm)	Average measured d (μm) Spray	Transitional	Rayleigh
CO_2-in-water injections										
127	0.00087	0.013	24.1	0.871	0.030	1.89	240	268	352	395
178	0.00085	0.013	24.1	0.871	0.025	1.89	336	276	298	483
254	0.00083	0.012	22.7	0.863	0.021	1.89	480	443	612	775
381*	0.00091	0.015	5.40	0.898	0.041	1.89	722	NA	617	1201
508	0.00084	0.012	23.3	0.866	0.015	1.89	958	NA	NA	1781
Water-in-CO_2 injections										
127	0.013	0.00085	23.9	1.002	0.070	1.90	242	127	327	344
254	0.012	0.00084	24.1	1.002	0.048	1.90	482	162	365	578
508	0.012	0.00081	21.9	1.002	0.042	1.88	957	NA	NA	1035
127 (Lee et al. 2003)					0.087	1.91	243	267		

* Injection was performed at 4 °C, resulting in higher viscosities and a lower interfacial tension. All other injections were performed at 10–12 °C.

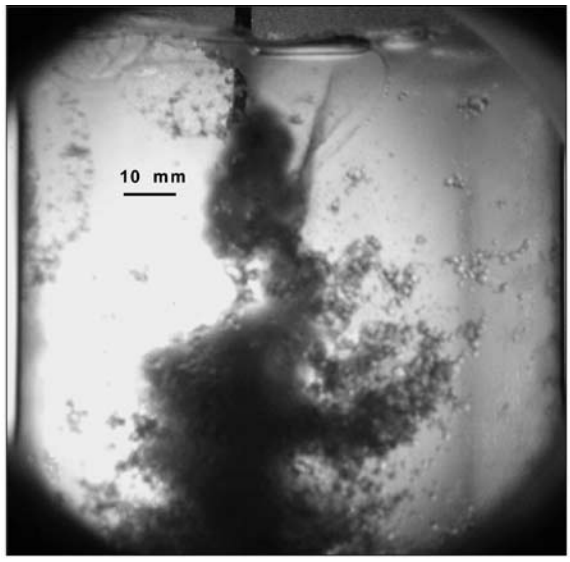

FIGURE 6. Visualization of CO_2 hydrate-covered water droplets formed when water is injected into liquid CO_2. Pressure = 5.6 MPa, temperature = 4.0 °C, capillary ID = 254 μm, injection flow rate = 10 mL/min (Rayleigh mode).

nesorge number vs. the Reynolds number for the water and liquid CO_2 systems under high-pressure conditions (Fig. 3). Under non-hydrate-forming conditions, measured drop sizes were somewhat larger but generally agreed with the calculation based on Rayleigh's maximum instability theory for both water-in-CO_2 and CO_2-in-water jet breakup in the Rayleigh regime. The observed droplet sizes were consistently smaller in the transitional and spray modes than in the Rayleigh regime (Table 2). The presence of hydrate did not appear to affect liquid-in-liquid breakup as long as the breakup time is shorter than the hydrate formation time (Teng and Zhao 1999). The confined space in a coflow injector (West et al. 2003; Lee et al. 2003), however, may promote droplet coalescence, yielding higher average size than that observed under spray mode. In comparing the two systems studied, the spray mode provided the smallest average droplet size, with the water-in-CO_2 drops being approximately 47% smaller than the CO_2-in-water spray droplets. This result makes injection of water into liquid CO_2 an attractive option to increase hydrate formation. With knowledge of the dynamics of

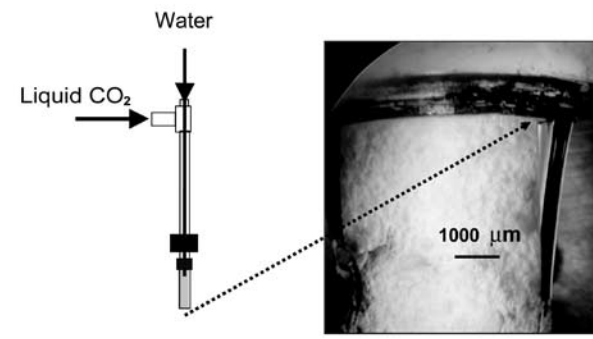

FIGURE 7. (**a**) Coflow injection system. (**b**) High magnification photograph of the liquid CO_2/water/CO_2 hydrate composite produced in liquid CO_2/water coflow injections (West et al. 2003).

jet breakup of water in CO_2, an injector design strategy can be developed. For example, we can estimate the drop size for Rayleigh mode to select an injector size and then use the relationship shown in Figure 3 to select the minimum flow rate necessary for spray mode (i.e., using the relationship $Z \cong 18\ Re^{-1}$).

Previous work using water-in-CO_2 injection in a liquid CO_2/water coflow injector (Fig. 7a) showed that by varying the water and CO_2 flow rates, certain hydrate conversions could be achieved that produced sinking particles of a liquid CO_2/water/CO_2 hydrate composite (West et al. 2003; Lee et al. 2003). Under experimental conditions equivalent to those in intermediate ocean depths (1000–1500 m), 19–24% conversion of liquid CO_2 to hydrate is required to produce a sinking particle plume (Holder et al. 1995; West et al. 2003). Injection experiments conducted at Monterey Bay, California, (Tsouris et al. 2004) have revealed that a conversion of 21–30% of liquid CO_2 into hydrate was achieved. Although this conversion was sufficient to produce negatively buoyant particles, it is highly desirable to increase the density of the particles, and thus the conversion of CO_2 to hydrate.

For any given flow rate, fine droplets can be achieved only by the spray breakup mode. Therefore, this mode is of the most interest in our experiments. When all the different capillaries are compared, it appears to be more effective to perform the injections using capillaries with smaller internal diameters because the spray breakup mode can be achieved at relatively low flow rates (Table 1). However, under spray mode, the drop size increase is small as capillary size doubled in the water-in-CO_2 experiments (Table 2). This effect suggests possible advantages

in using a larger-diameter injector, without a dramatic increase in droplet size (and, therefore, a reduction in reaction surface area), provided that the water is injected in the spray mode.

Additional knowledge of the dynamics of the CO_2-in-water system may also be beneficial to the development of injectors where CO_2 is injected directly into bulk ocean water (Holder et al. 1995; Brewer et al. 2002). In these injection schemes, minimizing the droplet size lowers the chances of CO_2 re-entering the atmosphere due to incomplete dissolution as the droplets rise. The relationship $Z \cong 18\ Re^{-1}$ (Fig. 3) appears to be valid for this system as well over a wide range of injector diameters (Tang et al. 2002). Therefore, this relationship could be used to determine the minimum injection flow rate to achieve spray mode for any injector diameter in direct ocean CO_2 injection as well.

This further understanding of the hydrodynamics of CO_2-in-water and water-in-CO_2 may result in a development of a wide range of phase contact applications, particularly in the conversion of CO_2 to hydrate as a strategy for carbon sequestration in the ocean.

ACKNOWLEDGMENTS

We gratefully acknowledge support from the Ocean Carbon Sequestration Program, Office of Biological and Environmental Research, U.S. Department of Energy (DOE), grant no. KP120203, under Contract No. DE-AC05-00OR22725 with UT-Battelle, LLC. The authors are thankful to M.K. Savage for editing the manuscript. M. Gborigi was supported by the Biological and Environmental Research Program for Minority Institutions administered by the Oak Ridge Institute of Science and Education.

REFERENCES CITED

Adams, E.E., Golomb, D.B., and Herzog, H.J. (1995) Ocean disposal of CO_2 at intermediate depths. Energy Conservation Management, 36, 447–452.

Ametistova, L., Twindell, J., and Briden, J. (2002) The sequestration switch: removing industrial CO_2 by direct ocean absorption. The Science of the Total Environment, 289, 213–223.

Aya, I., Yamane, K., and Nariai, H. (1997) Solubility of CO_2 and density of CO_2 hydrate at 30 MPa. Energy, 22, 263–271.

Brewer, P.G., Friederich, G., Peltzer, E.T., and Orr, F.M. Jr. (1999) Direct experiments on the ocean disposal of fossil fuel CO_2. Science, 284, 943–945.

Brewer, P.G., Peltzer, E.T., Friederich, G., and Rehder, G. (2002) Experimental determination of the fate of rising CO_2 droplets in seawater. Environmental Science and Technology, 36, 5441–5446.

Chun, B-S. and Wilkinson, G.T. (1995) Interfacial tension in high-pressure carbon dioxide mixtures Industrial and Engineering Chemistry Research, 34, 4371–4377.

Holder, G.D., Gugini, A.V., and Warzinski, R.P. (1995) Modeling clathrate hydrate formation during carbon dioxide injection into the ocean. Environmental Science and Technology, 29, 276–278.

Kitamura, Y., Mishima, H., Takahashi, T. (1982) Stability of jets in liquid-liquid systems. The Canadian Journal of Chemical Engineering, 60, 723–731.

Kleypas, J.A., Buddemeier, R.W., Archer, D., Gattuso, J.-P., Langdon, C., and Opdyke, B.N. (1999) Geochemical consequences of increased atmospheric carbon dioxide on coral reefs. Science, 284, 118–120.

Lee, S-Y., Liang, L., Riestenberg, D.E., West, O.R.., Tsouris, C., and Adams, E. (2003) CO_2 hydrate composite for ocean carbon sequestration. Environmental Science and Technology, 37, 3701–3708.

Lemmon, E.W., McLinden, M.O., and Friend, D.G. (2003) Thermophysical Properties of Fluid Systems. In P.J. Linstrom and W.G. Mallard, Eds., NIST Chemistry WebBook, NIST Standard Reference Database Number 69. National Institute of Standards and Technology, Gaithersburg, Maryland, (http://webbook.nist.gov).

Medina, M-G., Bond, G.M., and Stringer, J. (2001) An overview of carbon dioxide sequestration. Interface, 10, 26–30.

Meister, B.E. and Scheele, G.F. (1969) Drop formation from cylindrical jets in immiscible liquid systems. AIChE Journal, 15, 700–706.

Ormerod, W.G., Freund, P., and Smith, A. (2002) Ocean Storage of CO_2. 27 p. IEA Greenhouse Gas R&D Programme. Paris, France.

Phelps, T.J., Peters, D.J., Marshall, S.L., West, O.R., Liang, L., Blencoe, J.G., Alexiades, V., Jacobs, G.K., Naney, M.T., and Heck Jr., J.L. (2001) A new experimental facility for investigating the formation and properties of gas hydrates under simulated seafloor conditions. Review of Scientific Instruments, 72, 1514–1521.

Seibel, B.A. and Walsh P.J. (2001) Potential impacts of CO_2 injection on deep-sea biota. Science, 294, 379–380.

Siegenthaler, U. and Sarmiento, J.L. (1993) Atmospheric carbon dioxide and the sea. Nature, 365, 119–125.

Sloan, E.D. (1998) Clathrate Hydrates of Natural Gases. Marcel Dekker, Inc. New York NY.

Tang, L., Gorgas, T.J., and Masutani, S.M. (2002) Liquid CO_2 droplet spectra. Proceedings of the Sixth International Conference on Greenhouse Gas Control Technologies.

Teng, H. and Zhao, T.S. (1999) Influence of interfacial mass transfer and chemical reaction on breakup of low-solubility fluid jets in water. International Communications on Heat and Mass Transfer, 26, 177–185.

Teng, H., Kinoshita, C.M., and Masutani, S.M. (1995) Prediction of droplet size from the breakup of cylindrical liquid jets. International Journal of Multiphase Flow, 21, 129–136.

Tsouris, C., Brewer, P.G., Peltzer, E.T., Walz, P., Riestenberg, D., Liang, L., and West, O.R. (2004) Hydrate composite particles for ocean carbon sequestration: field verification. Environmental Science and Technology, 38, 2470–2475.

Tyler, E. (1933) Instability of liquid jets. Philosophical Magazine, 16, 504–518.

Uchida, T., Ebinuma, T., Kawabata, J., and Narita, H. (1999) Microscopic observations of formation processes of clathrate-hydrate films at an interface between water and carbon dioxide. Journal of Crystal Growth, 204, 348–356.

U.S. Department of Energy (1999) Carbon Sequestration Research and Development; Office of Science and Office of Fossil Energy, Washington, D.C.

Watson, R.T. (2001) Climate Change 2001: Synthesis Report, 34 p. Intergovernmental Panel on Climate Change Third Assessment Report. Cambridge University Press, Cambridge, U.K.

Weber, C. (1931) Disintegration of a liquid jet. Journal of Applied Mathematics and Physics, 11, 136–154.

West, O.R., Tsouris, C., Liang, L., Lee, S-Y., and McCallum, S.D. (2003) Negatively buoyant CO_2-hydrate composite for ocean carbon sequestration. AIChE Journal, 49, 283–285.

Yamasaki, A., Wakatsuki, M., Teng, H., Yanagisawa, Y., and Yamada, K. (2000) A new ocean disposal scenario for anthropogenic CO_2: CO_2 hydrate formation in a submerged crystallizer and its disposal. Energy, 25, 85–96.

MANUSCRIPT RECEIVED OCTOBER 1, 2003
MANUSCRIPT ACCEPTED FEBRUARY 4, 2004
MANUSCRIPT HANDLED BY BRYAN CHAKOUMAKOS